RSC Advances



This is an *Accepted Manuscript*, which has been through the Royal Society of Chemistry peer review process and has been accepted for publication.

Accepted Manuscripts are published online shortly after acceptance, before technical editing, formatting and proof reading. Using this free service, authors can make their results available to the community, in citable form, before we publish the edited article. This Accepted Manuscript will be replaced by the edited, formatted and paginated article as soon as this is available.

You can find more information about *Accepted Manuscripts* in the **Information for Authors**.

Please note that technical editing may introduce minor changes to the text and/or graphics, which may alter content. The journal's standard <u>Terms & Conditions</u> and the <u>Ethical guidelines</u> still apply. In no event shall the Royal Society of Chemistry be held responsible for any errors or omissions in this *Accepted Manuscript* or any consequences arising from the use of any information it contains.



Malachite Green interacts with membrane skeletal protein, spectrin

Malay Patra^a, Chaitali Mukhopadhyay ^a & Abhijit Chakrabarti* ^b

^aChemistry Department, University of Calcutta, Kolkata 700009, ^bCrystallography & Molecular Biology Division, Saha Institute of Nuclear Physics, Kolkata 700064, India

Corresponding Author

Prof. Abhijit Chakrabarti, PhD

E-mail: abhijit.chakrabarti@saha.ac.in

Tel.: 0091-33-2337-5345-49 (Extn.-1307); Fax: 0091-33-2337-4637

Running title: Malachite green binds to spectrin.

Abstract:

Malachite green (MG) is a triarylaminethane dye that has been extensively used in chemotherapy, and photochemotherapy for cancer treatment. We have examined the molecular interaction of the membrane skeletal protein with MG using biophysical and spectroscopic methods under physiological conditions. Fluorescence, both steady-state, synchronous and timeresolved and circular dichroism (CD) spectroscopy techniques aided with molecular docking studies were done to characterize the binding site (s), estimate the binding affinity and understand the molecular mechanism involved in the binding. MG caused quenching of intrinsic tryptophan fluorescence of both forms of dimeric erythroid and tetrameric non-erythroid spectrin with a binding stoichiometry of 1 MG per spectrin both in their dimeric and tetrameric forms indicated the common self-associating domain of spectrin to provide the unique binding site for the hydrophobic dye. The thermodynamic parameters associated with the binding showed involvement of van der Waals interactions and strong hydrophobic forces without largely affecting the secondary structure of the proteins. Results of this work have also indicated spectrin based cytoskeletal network as a chemotherapeutic target for cancer treatment like other cytoskeletal protein.

Keywords: Malachite green, Erythroid & Non-erythroid spectrin, Fluorescence, Molecular Docking.

Abbreviations:

MG, Malachite green

PMSF, phenyl methylsulfonyl fluoride

DTT, dithiothreitol

EDTA, ethylene diamine tetraacetic acid

EGTA, ethylene glycol tetraacetic acid

SDS, Sodium dodecyl sulfate

CD, Circular dichroism

SEM, Standard error of mean

SH3, Src homology domain 3

OPLS, Optimized Potentials for Liquid Simulations

Introduction:

Malachite green (MG) belongs to the tripheylmethane dyes which have been widely used as a novel therapeutic agent for both chemotherapy and photochemotherapy in neoplastic disease¹. The conceptual basis for the development of the therapeutic strategy has been based on the inner transmembrane potentials of both plasma and mitochondrial membrane. Because transmembrane potential is negative on the inner side of the both plasma and mitochondrial membranes, extensive conjugation with dye molecules displaying appropriate structural features are electrophoretically driven though the membranes and accumulate in the cytosol and inside the mitochondria. 1-6 The higher mitochondrial membrane potential, typical of tumor cells, thus opens up window for the selective destruction of these cells via mitochondrial targeting. Another type of structurally diverse anticancer drug functions as anti amyloid dye, has been considered for chemotherapy. 7-8 Often the anticancer drugs have been targeted to cytoskeletal proteins acting as chemotherapeutic target. 9-12 Recent study on actin cytoskeleton and its regulatory proteins have demonstrated that they could be selectively targeted in cancer chemotherapy. 13-15 Experimental data suggest that the relative levels of monomeric and polymeric actin in cells might be important for identifying the risk factors in certain cancer. ¹⁶ MG has also been shown to act as catalyst and interact with both DNA and RNA. 17-21 Oligonucleotide sequence containing guanine-rich stretches could from mutually hydrogen bonded, internally folded or internal strand G-quadruplex, which were better acceptor of MG and could bind RNA through stacking and electrostatic interactions. ^{22, 23} Such MG interactions have helped in the development of RNA aptamer-based biosensor for diagnostic and also for the use of RNA as the drug target. 18, 24 It was particularly important to study the MG interactions of proteins since it also interacted with BSA, hemoglobin and lysozyme.²⁵⁻²⁷ Recent studies also showed that tripheylmethane dye could cross blood-brain barrier to inhibit neurotoxicity of amyloid β -peptide by generating nontoxic aggregates and activated β -arrestin which regulates the signaling of G-protein couple receptor.^{28,29} MG and its derivatives were also absorbed by lipid membrane leading to change of morphology of lipid vesicles.³⁰

Besides, the use of MG in chemotherapy for cancer treatment, it has been employed as antifungal agent in animal food and fish industry due to its excellent ability to control the protozoa infection and some other diseases in aquatic species.^{31, 32} However, MG is a controversial chemical due to its carcinogenic, genotoxic, mutagenic and teratogenic properties in human.³³ Earlier studies confirmed that MG could induce oxidative DNA damage and inhibit intracellular enzyme action through free radical mechanism.³⁴ Histopathology study has demonstrated MG's detrimental effects in liver, gill, kidney, intestine and pituitary gonadotropic cells and in the eyes of rabbits leading to sight hyperemia.³⁵ Even though the use of the dye has been banned in several countries (USA and Europe), it has been still being used in many part of the third world countries due to its high efficiency and low cost.³⁶ It was therefore, necessary to investigate the mode of action of MG and finding out secondary protein targets, as it could provide valuable insight into the mechanism of drug toxicity.

Spectrin is the major constituent of membrane skeleton of eukaryotic cells and forms a filamentous intracellular network that acts as a scaffold for cytoplasmic proteins. The inherent flexibility of spectrin is an important factor in elastic deformability of cells like erythrocytes, an essential requirement for the passage of these cells in circulatory system. Spectrin is an elongated heterodimer with large molecular mass of 520,000 Daltons. The two subunits, α - and

β-spectrin associated laterally through the carboxy terminal of α spectrin and amino terminal of β-spectrin to give 100 nm long rod shaped heterodimer molecule. There are two forms of spectrins, the erythroid and non-erythroid bearing a high sequence homology between them. Despite its high sequence similarity with erythroid spectrin, two spectrin isoform are quiet different in terms of structure and function. Recent crystallographic studies reveal that the tetramerization site or self associating domain of non-erythroid spectrin α-spectrin is different from that of erythroid spectrin, supported by the fact that non-erythroid spectrin forms tetramer about 15 times stronger than that of the erythroid spectrin. Non-erythroid spectrin has been shown to be more rigid and thermally stable than erythroid spectrin and also interacts strongly with anionic membrane than the erythroid spectrin.

Several recent reports have implied that spectrin, in addition to their main structural and mechanical support to the membrane bilayer could have other functions in regulatory and signal transduction pathways in fibroblasts, neurons, muscle cells and lymphocytes. ⁴⁶⁻⁴⁸ Among many domains responsible for interactions with membrane and membrane attachment proteins, spectrin possesses two domains which are involved in regulatory and signaling pathways. SH3–Src protein tyrosine kinase homology domain, which is present in many proteins engaged in cell signaling and mediates interactions with proline-rich stretches in a number of target proteins, is mostly found in α-spectrin and located also to the C-terminal segment of some β-spectrin isoforms, first resolved in pleckstrin. ⁴⁹⁻⁵¹ Observation of spectrin in various myeloid and lymphoid cell lines revealed appearance of two patterns of spectrin distribution. In most cell lines spectrin was evenly distributed in the cytoplasm, but in some other the cells contained spectrin aggregates. ⁵² Recruitment of intracellular proteins to the plasma membrane is well

Page 7 of 43

known for the initiation of signal transduction events, and participation of spectrin in this phenomenon may indicate its signaling function in lymphocytes. Most of the recent studies concerning participation of spectrin in apoptosis concentrate on appearance of calpain and caspase generated breakdown products of spectrin. 53-56 During apoptotic and necrotic cell death, the plasma membrane undergoes several changes, including loss of sialic acid residues from glycoproteins, loss of microvilli, and cell-cell junctions, and loss of phospholipid asymmetry, which can be detected by the exposure of phosphatidylserine (PS) at the outer plasma membrane leaflet. 57-59 These deformations are predominantly associated with degradation of membrane and cytoskeletal proteins including apoptotic proteolysis of non-erythroid spectrin. 59-61 A previous study indicates that spectrin aggregated in early apoptotic lymphoid and leukemic cells isolated from the blood of patients after 24 h of ongoing chemotherapy. Spectrin also binds antitumor antibiotics, mithramycin, and chromomycin A₃ with a higher affinity than that of DNA and such interactions also led to change in the tertiary structure of the protein 62 and earlier study by Dubielecka and coworkers showed that spectrin could bind DNA binding anticancer agent Mitoxantrone and binding of such anticancer drug could alter the spectrin phospholipid interactions. 63, 64

Like other cytotoskeletal proteins, spectrin plays a crucial role in cell division, signal transduction between intracellular and extracellular compartments and apoptotic cell death. ⁵⁶⁻⁵⁹ However, no spectrin inhibitor has been developed till recently when they were selectively targeted in cancer chemotherapy. ⁶⁰ In order to know how these drugs affect the spectrin based membrane skeleton, we've found that MG binds to spectrin. We've characterized the binding, evaluated the thermodynamic parameters associated with it, established the structure–function relationship and the pharmacophoric attachment to the target, which could help in designing

better chemotherapeutic drugs. We have previously utilized tryptophan fluorescence of spectrin to monitor interactions with different drug molecules e.g. local anesthetics dibucaine, tetracaine, anticancer antibiotics and hydrophobic ligands e.g. heme, protoporphyrin and ATP causing quenching of tryptophan fluorescence. ⁶³⁻⁶⁸ In the present study, we have examined the binding of MG to purified spectrin and have identified a unique binding site in both erythroid and non-erythroid forms of spectrin at the self-associating domain using fluorescence spectroscopy and molecular docking techniques. Acrylamide quenching and circular dichroism studies also indicated conformational changes induced by binding of MG. Thermodynamic parameters showed the binding to be associated with a large positive change in entropy indicating the mode of binding to be predominantly hydrophobic in nature.

Materials and Methods:

Isolation and purification of erythroid and non-erythroid spectrin:

White ghosts from ovine blood, obtained from local slaughter house, were prepared by hypotonic lysis in 5mM phosphate, 1mM EDTA containing 20 µg/ml of PMSF at pH=8.0 (lysis buffer) following the published procedure.^{39, 66} Spectrin dimers were purified from the published protocol that is elaborated our earlier work. Erythroid spectrin was finally purified after the concentrate by 30% ammonium sulphate precipitation followed by chromatography on Sepharose CL-4B. Spectrin was stored in a buffer containing 5 mM phosphate, 20 mM KCl, 1mM EDTA pH=8.0 containing 0.2 mM DTT. Before all the fluorescence experiment the protein was dialysis extensively against the buffer containing 10 mM Tris-HCl 20 mM KCl pH=7.8 to removed the DTT. The purity of spectrin preparation was checked by 7.5% SDS-poly acrylamide gel electrophoresis under reducing condition showing the characteristic bands of spectrin dimer

after Coomassie blue stain shown in Figure-S1. The concentration of spectrin was determined spectrophotometrically using the absorbance of 10.7 at 280 nm for 1% spectrin.

Non-erythroid spectrin in its tetrameric from was purified from ovine brain, obtained from local slaughter house, following published procedure.^{39, 41} Fresh homogenized brain was further homogenized in 10 mM Tris at pH=8.0 containing 5mM MgCl₂ 1mM EGTA 0.2 mM DTT and 0.2mM PMSF and pH of the solution readjusted to 8 from 1M Tris base. The salt concentration of the solution was maintained at 0.6M from stock NaCl solution and was stirred for 1hr at 4°C. After centrifugation at 15000g the supernatant passed through the cheese cloth. The crude non-erythroid spectrin obtained after centrifugation at 12000g at 4°C. Purified non-erythroid spectrin after concentrating with 50% ammonium sulphate precipitation and followed by chromatography on Sepharose CL-4B. Purity of the preparation was checked by 8% SDS poly acrylamide gel electrophoresis under reducing condition, also shown in Figure-S1. Non-erythroid spectrin concentration was determined by Bradford method with bovine serum albumin as a standard.

Fluorescence measurements:

Steady state fluorescence measurements were performed Cary Eclipsed (Varian) fluorescence spectrophotometer equipped with a thermostatic cell holder and 1cm path length quartz cuvette. Quenching experiments were performed in a buffer containing 10 mM Tris 20 mM KCl pH=7.8 keeping the concentration of both spectrin fixed at 0.1mg/ml varying MG concentration from 0 to 25 μ M. The excitation and emission silt were set at 5nm each, intrinsic fluorescence was obtained by exciting spectrin solution at 295 nm selectively excited Trp residue and the fluorescence emission spectra were recorded between 310 to 400 nm. Fluorescence

intensities were corrected for the inner filter effect, due to absorption of the protein and the MG, when absorbance, at both excitation and emission wavelengths, of the samples exceeded 0.05.^{67,68}

Fluorescence anisotropy (r) measurements were performed using a Cary Eclipsed (Varian) polarization accessory in a pH=7.8 Tris-HCl buffer solution at room temperature. Anisotropy values were calculated from the fluorescence intensity measurement a vertical excitation polarizer and vertical and horizontal emission polarizer according to the equation. ⁶⁷

$$r = I_{VV} - GI_{VH} / I_{VV} + 2GI_{VH}$$
 (1)

where I_{VV} and I_{VH} are the measured fluorescence intensities, with excitation polarizer vertically oriented and emission polarizer vertically and horizontally oriented. G is the grating correction factor and is equal to I_{HV}/I_{HH} .

Fluorescence lifetime were measured from the time resolved intensity decay by time correlated single photon counting method (TCSPC) method using Fluromax-3 (JY-Horiba) fluorescence spectrophotometer. A nanosecond diode laser as the light source at 295 nm was applied to selectively excited spectrin and the emission monitored at 340 nm. To optimize the signal to noise ratio, 5,000 counts were collected in the peak channel. All the experiments were performed using the excitation and emission silt 2 and 3 nm respectively. DAS6 soft ware used to deconvolute the fluorescence decays and the mean (average) lifetime's < τ >for tri-exponential decays of fluorescence were calculated from the decay times and preexponential factors using the following equation.

$$\langle \tau \rangle = \alpha_1 \, \tau_1^2 + \alpha_2 \, \tau_2^2 + \alpha_3 \tau_3^2 / \alpha_1 \tau_1 + \alpha_2 \tau_3 + \alpha_3 \tau_3 \tag{2}$$

Where α_i and τ_i represent the amplitude and times of decay components such that Σ_i α_i =1. The goodness of fit was estimated by using χ^2 values.

Stern Volmer quenching:

Fluorescence quenching refers to any process that decreases the fluorescence intensity of a fluorophore. A variety of molecular interaction takes place during quenching of a sample such as excited electron transfer, ground state complex formation and collisional quenching. Fluorescence quenching has been analyzed using following well known stern volmer equation:

$$F_0/F = 1 + K_{sv}[Q]$$
 (3)

Where F_0 and F are the relative fluorescence intensities in the absence and presence of quencher respectively, K_{sv} is the Stern Volmer constant and [Q] is the concentration of the quencher and $K_{sv} = k_q \, \tau_0$ where k_q is the bimolecular quenching rate constant and τ_0 is the average life of protein in the absence of dye.

Experiment on quenching of tryptophan fluorescence were carried out by excitation at 295 nm and recorded emission intensities at 340 nm, after serial addition of small aliquot of acrylamide stock solution. ^{68, 69} Corrections were applied to the observed intensities for dilution of the protein and absorbance for the incident light by acrylamide. Both proteins (0.1mg/ml) were incubated with 100 times concentrate MG before quenching experiment are carried. Quenching constant was analyzed by fitting of the Stern Volmer equation.

Circular Dichroism spectroscopy:

Far UV-CD measurements were performed on a Biologic CD spectrophotometer (MOS 450) in a 0.1cm path length cell at room temperature. For monitoring changes in secondary structure changes, all spectra were recorded in 0.5 nm wavelengths increment in the far UV changes from 190 nm to 250 nm. Five scans were accumulated for each spectrum taking the average as the final data corrected by subtraction of appropriate blank without protein. Both proteins (0.2mg/ml) in a buffer of 10 mM 20 mM KCl, pH 7.8 was incubated 1 hour with 100 times concentrate of MG before the spectra were recorded. They were smoothed within the permissible limits by the in-built software in the instruments. The results were expressed as the mean residue ellipticity (MRE) in deg cm² mol⁻¹ which defined as -

$$MRE= [\theta]_{obs} M / 10.1.c$$
 (4)

Where θ_{obs} is the CD mill degrees, M is the molecular weight of the protein in g dmol⁻¹, 1 is the path length of the cuvette and c is the concentration of protein in g/L.

Quantitative assessment of the percentage of α -helix in spectrin in the presence and absence of MG can be estimated by the relation. ^{70,71}

% of
$$\alpha$$
-helix= $[\theta]_{222}+2340/-30300$ (5)

Analysis of binding data:

Results from fluorometric titration were analyzed by the following method. The apparent dissociation constant (K_d) were determined using a non linear curve fitting analysis to equations 7 and 8. All experiments points for binding isotherms were fitted by list square analysis. ^{63, 66, 67}

$$K_{d} = \left[C_{SP} - (\Delta F/\Delta F_{max}) \times C_{SP}\right] \times \left[C_{MG} - (\Delta F/\Delta F_{max}) \times C_{SP}\right] / (\Delta F/\Delta F_{max}) \times C_{SP}$$
(6)

$$C_{SP} \cdot (\Delta F/\Delta F_{max})^{2} - (C_{SP} + C_{MG} + K_{d}) \cdot (\Delta F/\Delta F_{max}) + C_{MG} = 0$$
(7)

 ΔF is the change in fluorescence intensity at 340 nm for each point of titration curves. ΔF_{max} is the same parameter when ligand is totally bound to protein. C_{MG} is the concentration of malachite green; C_{SP} is the concentration of the protein and K_d is the apparent dissociation constant.

A double reciprocal plot was used for determination of ΔF_{max} using

$$1/\Delta F = 1/\Delta F_{\text{max}} + 1/\left[K_{\text{app}} \cdot \Delta F_{\text{max}} \left(C_{\text{MG}} - C_{\text{SP}}\right)\right] \tag{8}$$

The linear double reciprocal plot of 1/ ΔF against 1/ (C_{MG} – C_{SP}) is extrapolated to ordinate to obtained value of ΔF_{max} .

When small molecules bind independently to a set of equivalent binding sites on a macromolecules the binding also calculated by the method according to the method of Lissi and Abuin. 12,25,26,27,72

$$\log (F_0 - F)/F = \log K + n \log [Q]$$
(9)

$$\log (F_0 - F) / F = n \log K - n \log 1 / [Q_t] - (F_0 - F / F_0) [P_t]$$
(10)

Where F_0 and F are the fluorescence intensities in the absence and presence of quencher, respectively, K and R are the association constant and the number of binding sites respectively, R and R are the total concentration of quencher and protein respectively.

The effect of ionic strength on the binding of MG with erythroid and non-erythroid spectrin was determined by increasing the concentration of sodium chloride from 20 mM to 200 mM in Tris-HCl buffer by fluoremetric titration at 25°C as given above. Erythroid, non-erythroid spectrin and MG concentration were used in the same concentration as in the quenching studies and using appropriate blank.

Evaluation of thermodynamic parameters:

Thermodynamic parameters, ΔH (van't Hoff enthalpy), ΔS (entropy), and ΔG (free energy), were determined using the equations

$$\ln K_{app} = -\Delta H/RT + \Delta S/R \tag{11}$$

$$\Delta G = \Delta H - T \Delta S \tag{12}$$

R and T are the universal gas constant and absolute temperature respectively. K_{app} (apparent dissociation constant) were determined from the previous equation. ΔH and ΔS were determined from the slope and intercept of a plot ln K_{app} against 1/T. ΔG was determined from the equation 12 after incorporation of ΔH and ΔS value obtained from equation 11.

Molecular docking study:

Molecular docking studies were carried out to elucidate the binding of MG with different structural domain of erythroid spectrin. As the crystal or NMR structures of intact dimeric spectrin are not available, we built the homology model of different domain of spectrin by using Modweb (http://modbase.Combio.uccsf.edu/ModWEB20html/Modweb.html). The amino acid sequences of different domains of erythroid spectrin are taken from SWISS PROT. The self-association domain of non-erythroid spectrin and SH3 domain of erythroid spectrin were created

using the structure of self-association domain erythroid (3LBX, pdb) and non-erythroid spectrin SH3 domain (1NEG.pdb) as the template structure. The other domains of the spectrin, such as self association domain of spectrin (3LBX.pdb) and α-N terminal region of erythroid (10WA.pdb) of non-erythroid spectrin (3F31.pdb) and SH3 domain of non-erythroid spectrin (1NEG.pdb) and ankyrin-binding domain of erythroid (3f57A.pdb) of non-erythroid spectrin (3edvA.pdb), were studied using their respective crystal or NMR structure. Energy minimizations of the models were performed using GROMACS OPLS force field. ⁷³ For docking study of MG with different structural domain of spectrin, three dimensional structures of the ligand obtained from their PDB (3btl.pdb) structural data base. Docking study was performed with Auto Dock 4.2 software package to calculate the interaction between ligand and different domain of spectrin. Auto dock uses the Lamarckian genetic algorithm to calculate possible conformer of the hydrophobic ligand that binds different domain of spectrin. 74, 75 To recognize the binding site in spectrin, blind docking was carried out, the size set to 80, 75 & 60 along X-, Y- and Z-axes, with 1.00Å grid spacing. During docking a maximum number of 10 conformers was used for each domain and the lowest binding energy molecule undergoes further analysis. The lowest energy binding domain was visualized using PyMOL Molecular graphics system. ⁷⁶

Results and Discussion:

Malachite green induced fluorescence quenching of erythroid and non-erythroid spectrin:

Fluorescence spectroscopy is the most effective method to study the interaction of small ligand molecules with macromolecules. Binding of MG with erythroid and non-erythroid spectrin was monitored by following quenching of relative intensity of tryptophan fluorescence of both forms of spectrin upon excitation at 295 nm. Fig 1 shows the fluorescence emission

spectra of dimeric erythroid and tetrameric non-erythroid spectrin in absence and presence of MG. It could be seen in Fig 1 that spectrin exhibits emission maximum at 338 nm, in the absence of MG. Beyond 50% decrease in the fluorescence intensity, the emission maxima shift towards longer wavelength of 345 nm indicating structural changes due to interaction of MG with spectrin leading to a decrease in the hydrophobicity of the the microenvironment of the tryptophan residues in both forms of spectrin.

The mechanism of fluorescence quenching is generally of two types, static (by complex formation) and dynamic (collisional processes), which could be distinguished by their dependence on temperature and viscosity. In case the former with rise in temperature, the stability of the formative compound will be lowered. On the other hand, in dynamic quenching, the effective number of colliding ions increases, enhancing the transfer of energy and thereby quenching constant of the fluorescence substance with rise in temperature. From the Stern-Volmer plots of F_0/F Vs [MG] at three different temperatures, shown in Fig 2, it is evident that the mechanism of quenching is static in nature since it does not show significant dependence on temperature. The corresponding K_{SV} and k_q values were found to decrease with increasing temperature, summarized in the Table S1 of supporting information, further indicate the mode of quenching of spectrin by MG to be static in nature. 77,78

Evaluation the binding affinity:

Binding parameters were determined from decrease in fluorescence intensity of spectrin upon addition of increasing concentrations of MG. $^{63, 66, 67}$ The representative binding isotherms for the binding of MG with both forms of spectrin are shown in Fig 3. The insets of Fig 3 show the representative double reciprocal plots of $1/\Delta F$ against $1/(C_L - C_S)$ to evaluate ΔF_{max} and the apparent binding constant. The nature of binding isotherms and linear double reciprocal plots

suggest non-cooperative mode of interaction and the binding dissociation constant for spectrin/MG interactions are summarized in Table 1.

The binding constant was also evaluated using the equation (10) to estimate the number of binding site involve in the binding reaction. $^{12, 26, 72}$ The K_d and number of binding site (n) were found to be $15\pm4~\mu\text{M}$ and 0.88 respectively (Fig 3). Results show that K_d values, estimated by three different methods, are comparable, summarized in Table 1. The trend of decreasing binding constant values with increasing temperature, similar to those observed with K_{SV} values, further support the MG induced quenching of spectrin fluorescence to be static in nature.

Estimation of the thermodynamic parameters:

The interaction force between small molecule and macromolecules mainly include four types; hydrogen bonding; hydrophobic interaction; ionic electrostatic interaction and van der walls force. Thermodynamic parameters, free energy change (ΔG), enthalpy change (ΔH), and entropy change (ΔS) can provide evidence for classifying interaction modes. Usually if the enthalpy changes ΔH do not vary prominently over the temperature range studied, the data can then be estimated from van't Hoff's equation (eq 11). From the linear relationship between ln K_a and 1/T the thermodynamic parameters were obtained (Table 2). The negative change in ΔG indicates the spontaneity of the process of formation of the macromolecules—ligand complex, which is an exothermic in nature accompanied by positive ΔS (Fig 4). Ross and co-worker have characterised the sign and magnitude of thermodynamic parameters associated with various types of interactions those may take place in the process of association.⁷⁹ For typical hydrophobic effect both ΔH and ΔS are positive, while they are negative for van der Waals forces and hydrogen bond formation in low dielectric medium. Further, specific electrostatic interactions between ionic species in aqueous medium were expressed by a positive ΔS value

and a small negative or almost zero value of ΔH . A negative ΔH value is observed whenever there are hydrogen bonds in the binding events as seen in MG-spectrin interactions with negative ΔH and positive ΔS value for both forms of spectrin (Table 2). Taken together with the negative ΔH and positive ΔS it suggests that hydrophobic interactions and hydrogen bonding together contribute to the stability of the MG-spectrin complex.

The effect of ionic strength was also studied by increasing the ionic strength of the buffer by addition of NaCl (0.2-2M). It was observed (Table S2) that K_d decreased with increasing ionic strength of the buffer suggesting the hydrophobic interactions to dominate the MG-spectrin interaction. Table 1 summarizes the K_d and binding stoichiometry values for MG-spectrin interactions.

Synchronous Fluorescence spectroscopy:

The conformational changes of dimeric erythroid and tetrameric non-erythroid spectrin in presence of MG were studied by synchronous fluorescence spectroscopy that involves simultaneous scanning of excitation and emission monochromators, maintaining a constant wavelength interval between them. The synchronous fluorescence spectroscopy gives information about the environment in the vicinity of a fluorophore such as Trp and Tyr in case of proteins. This method has several advantages such as spectral simplification and reduction of spectral band width, avoiding differential perturbation. It has been reported that the shorter difference in wavelength ($\Delta\lambda$ =15) signifies the microenvironment of Tyr residues and longer difference in wavelength difference ($\Delta\lambda$ =60) indicate microenvironment around the Trp residues. Few representative synchronous fluorescence spectra of erythroid and non-erythroid spectrin are shown in the Fig 5. The wavelength of maximum emission of Trp was red-shifted only by 3 nm suggesting that the polarity around the Trp residues in both the forms

remained almost unaltered in presence of MG. However, stronger fluorescence quenching is also observed upon addition of MG indicating the proximity of the MG binding site near the Trp residues.

Fluorescence lifetime analysis:

Static and dynamic quenching could be distinguished through their differences in the dependence of temperature and also by time-resolved fluorescence measurements.⁶⁸ The fluorescence lifetime data of both forms of spectrin, in presence and absence of MG are summarized in the supporting information Table S3. The decay profiles were fitted with three exponentials with the relative fluorescence lifetime (τ_1) 1.26 ns, (τ_2) 4.32 and (τ_3) 0.143 for erythroid spectrin and (τ_1) 1.27 ns, (τ_2) 4.08 and (τ_3) 0.203 for non-erythroid spectin, respectively. The mean fluorescence lifetime of both forms of spectrin did not change significantly in presence of two different concentrations of MG showing that the fluorescence quenching essentially followed static mechanism again indicating ground-state complex formation between spectrin and MG.⁷⁸

Binding induced change in spectrin conformation:

Circular dichroism spectroscopy is a powerful technique to monitor the secondary structure alternation of a protein. CD spectra of erythroid and non-erythroid spectrin in the absence and presence of MG are shown in the Fig 6, showing two negative bands in the far UV region at 208 nm and 222 nm assignable to π - π * and n- π * transitions which carry signature of a typical α -helical protein. The ellipticity of both protein decreases slightly upon increasing the concentration of MG indicating loss of α -helical content in the proteins. The α -helical content of erythroid spectrin was calculated from the equation (5) which indicated a reduction of α -helical structure from 55% to 48% for spectrin: MG at a molar ratio 1:200. Similar result was also

obtained for the tetrameric non-erythroid spectrin suggesting that MG interacts with the hydrophobic amino acid residues of the protein and partially destroys the hydrogen bonding networks. Similar decrease of α-helical content in a protein upon binding of ligand molecule is also reported previously by various other group for Triazole fungicides -HSA adducts. All the above analysis revealed that the binding of MG induce minor but definite conformational changes in spectrin indicated by changes in the emission maxima, quenching of synchronous fluorescence and far-UV CD spectra which result better exposure of MG to the hydrophobic regions of the protein. The steady state fluorescence anisotropy for both forms of spectrin also decreases from 0.13±0.01 in absence of MG to 0.11±0.01 in the presence of it.

Stern Volmer fluorescence quenching:

The microenvironment in and around the Trp residues and their extent of accessibility by a neutral quencher was investigated by fluorescence. Quenching by acrylamide mainly takes place through a dynamic mechanism with physical interaction between fluorophore and the quencher. Stern Volmer plots for the acrylamide quenching of both erythroid and non-erythroid spectrin in the presence and absence of MG are shown in the Fig 7. It is clearly seen from the data given in Table 3 that the quenching constants, K_{SV} decrease significantly from 4.6 and 4.2 for erythroid and non-erythroid spectrin, respectively to 3.0 and 3.3 in presence of MG. This further indicates binding of MG to alter the accessibility of tryptophan to the quencher and binding induced conformational changes of both forms of spectrin in presence of MG.

Molecular docking study:

In order to understand the efficiency of MG as a therapeutic agent, it is necessary to explore the nature of binding site of MG in proteins. We have explored MG binding to spectrin on the basis of blind molecular docking simulation method. Spectrin subunits are assumed to

have flexible rod like morphology from extended array of triple helical motifs consisting about 106 amino acids. One could structurally define spectrin as a linear combination of actin binding domain, rod domain, containing repeats motif of the 3-helix bundle and self associating domain. The N-terminal domain of α-spectrin, the SH3 domain in the middle of the rod domain, the ankyrin binding domain of β -spectrin, and the self associating domain of both erythroid and nonerythroid spectrin were used for docking study. It has been previously shown that the hydrophobic ligand, Prodan bound to spectrin subunits with lower affinity compared to intact spectrin⁶⁶. Details of such docking studies have been given in our earlier work.⁷⁴ Different structural domain is created using Modweb server. One of the best docking results was obtained between MG with the SH3 domain of erythroid spectrin, reflected in the binding energies summarized in Table 4. Both experimental results and the positive binding energies, rule out the possibilities of the ankyrin binding domain and the N-terminal domain of α-spectrin, shown in supporting information Fig S2. Negative binding energy and low inhibition constant are calculated using Autodock 4.2 software package, indicating favorable binding interactions between the MG and spectrin. The experimental data and docking results together shows both the SH3 domain and the self-associating domain capable of accommodating MG, shown in Fig 8. The amino acid residues involved in the sphere of binding sites of MG are listed in supporting information Table S4. Thermodynamic parameters associated with the binding indicate the interactions not to be exclusively hydrophobic in nature. There are, however, several polar residues found in the vicinity of the bound MG, which could also contribute to the stability of the molecular complex via electrostatic and hydrogen bonding interactions. This is in good agreement with the experimentally determined thermodynamic parameters and the fact that the binding showed little effect on ionic strength of the medium. It could be seen that the SH3

domain and the self association domain could accommodate MG and the interactions being predominated by favorable contacts with hydrophobic amino acids (Table 5). In terms of ligand binding activities, SH3 domain is implicated only in the recognition of proline-rich peptides that involve conserved peptide-binding surface of SH3. Moreover, as the hydrophobic interactions are non-directional and non-specific, it has been reported earlier that good docking poses are poorly ranked, particularly when the interaction is predominantly hydrophobic, when the ligand makes very few electrostatic interactions with the protein. Molecular docking studies alone indicate that MG binds to the four major structural domains, following the order in the strength of binding to the SH3 domain > Self-association domain > N-terminal domain of α -spectrin >Ankyrin binding domain of non-erythroid spectrin. The binding experiments, particularly with the tetrameric non-erythroid spectrin, however, indicate a common, unique binding site for MG in the self association domain of spectrin.

Conclusion:

Malachite green, a triphenylmethane dye, continued to find roles as therapeutic tools despite concern about their cytotoxicity and environmental impact. Due to its structural features and selective phototoxicity toward tumor cells it has been utilized as medicine for cancer treatment. Recently, tripheylmethane dye variants have been used for the treatment of plaque forming diseases of the central nervous system.

In this work, we have explored studies on the interaction of MG, permeable to the blood brain barrier, with a major cytoskeletal protein using fluorescence spectroscopy and molecular docking approach. The spectroscopic data suggests that both erythroid and non-erythroid spectrin binds MG with a binding stoichiometry of 1 MG per spectrin, both in its dimeric and

tetrameric forms, indicating the self-association domain as the major binding site, only common site between both the dimeric and tetrameric spectrin. Far UV circular dichroism and synchronous and time-resolved fluorescence studies in presence of MG also indicate that both secondary and tertiary structural changes take place. Thermodynamic data show that the interaction is spontaneous and H-bonding, van der Waals type interactions play major role for stability of the MG-spectrin complex. Molecular docking study further indicated that the MG forms complexes with erythroid and non-erythroid spectrin through H-bonding and hydrophobic interactions and several amino acid residues take part in the process. Since spectrin plays an important role in the process of apoptotic cell death, the specific, moderately high binding affinity MG indicates spectrin based cytoskeletal network to have potential as a chemotherapeutic target for cancer treatment.

Acknowledgements: M.P. acknowledges the award of the Senior Research Fellowship from University Grants Commission (India). The work is funded by the MSACR project of Department of Atomic Energy, India.

References:

- 1. L. B. Chen, Annu. Rev. Cell Biol. 1988, (4) 155–181.
- S. Davis, M. J. Weiss, J. R. Wong, T. J. Lampidis, and L. B. Chen, J. Biol. Chem. 1985 (260) 13844–13850.
- S. D. Bernal, T. J. Lampidis, R. M. McIsaac and L. B. Chen, Science 1983 (222) 169– 172.

- 4. A. R. Oseroff, D. Ohuoha, G. Ara, R. J. McAuliffe, and L. Cincotta, Proc. Natl. Acad. Sci. U. S. A. 1986 (83) 9729–9733.
- 5. J. S. Modica-Napolitano, J. L. Joyal, G. Ara, A. R. Oseroff and J. R. Aprille, Cancer Res. 1990 (50) 7876–7881.
- 6. G. L. Indig, G. S. Anderson, M. G. Nichols, J. A. Bartlett, W. S. Mellon and F. Sieber, J. Pharm. Sci. 2000 (89) 88–99.
- 7. I. K. Kandela, J. A. Bartlett, and G. L. Indig, Phutochem. Photobiol. Sci. 2002 (1) 309-314.
- 8. G. L. Indig, Dev. Pure Appl. Chem. 1999 (3) 9–19.
- 9. E. J. Luna, and A. L. Hitt, Science. 1992 (258) 955–964.
- 10. M. A. Jordan, and L. Wilson, Curr. Opin. Cell. Biol. 1998 (10) 123–130.
- Q. Shi, K. Chen, S. L. Morris-Natschke, and K. H. Lee, Curr. Pharm. Des. 1998 (4)
 219–248.
- S. Chakraborti, L. Das, N. Kapoor, A. Das, V. Dwivedi, A. Poddar, G. Chakraborti, M. Janik, G. Basu, D. Panda, P. Chakrabarti, A. Surolia, and B. Bhattacharyya, J. Med. Chem. 2011(54) 6183–6196.
- C. Stournaras, E. Stiakaki, S. B. Koukouritaki, P. A. Theodoropoulos, M. Kalmanti, Y. Fostinis and A. Gravanis, Biochem. Pharmacol. 1996 (52) 1339–1346.
- H. L. Asch, K. Head, Y. Dong, F. Natoli, J. S. Winston, J. L. Connolly and B. B. Asch,
 Cancer. Res. 1996 (56) 4841–4845.
- 15. G. Dhar, D. Chakravarty, J. Hazra, J. Dhar, A. Poddar, M. Pal, P. Chakrabarti, A. Surolia and B. Bhattacharyya, Biochemistry 2015 (54) 1132-1143.

- G. P. Hemstreet, J. Y. Rao, R. E. Hurst, R. B. Bonner, P. Waliszewski, H. B. Grossman,
 M. Liebert and B. L. Bane, J. Cell. Biochem. 1996 (25) 197–204.
- 17. M. S. Baptista and G. L. Indig, J. Phys. Chem. B 1998 (102) 4678-4688.
- 18. D. M. Kolplaschikov, J. Am. Chem. Soc. 2005 (127) 12442-12443.
- 19. J. E. Sokoloski, S. E. Dombrowski and P. C. Bevilacqua, Biochemistry 2012 (51) 565-572.
- 20. J. B. D. Costa, A. I. Andreiev and T. Dieckmann, Biochemistry 2013 (52) 566-572.
- 21. J. B. D. Costa and T. Dieckmann, Mol. Biosyst. 2011 (7) 2156-2163.
- 22. A. C. Bhasikuttan, J. Mohanty and H. Pal, Angew. Chem. 2007 (119) 9465-9467.
- D. H. Nguyen, S. C. DeFina, W. H. Fink and T. Dieckmann, J. Am. Chem. Soc. (2002)
 124 15081-15084.
- 24. W. Xu and Y. Lu, Anal. Chem. 2010 (82) 574-578.
- Y. Z. Zang, B. Zhou, X. P. Zhang, P. Haung, C. Hong and Y. Liu, J. Hazard. Mater. 2009
 (163) 1345-1352.
- 26. W. Peng, F. Ding, Y. K. Peng and Y. Sun, Mol. Biosyst. 2013 (10) 138-148.
- F. Ding, X. N. Li, J. X. Diao, Y. Sun, L. Zhang, L. Ma, X. L. Yang, L. Zhang and Y. Sun, Ecotox. and Enviro. Safe. 2012 (78) 41-49.
- 28. H. E. Wong, W. Qi, H. M. Choi, E. J. Fernandez and I. Kwon, ACS. Chem. Neurosci. 2011 (2) 645-657.
- 29. L. S. Barak, Y. Bai, J. C. Snyder, J. Wang, W. Chen, and M. G. Caroon, Biochemistry 2013 (52) 5403-5414.
- 30. R. M. Uda, E. Hiraishi, R. Ohnishi, Y. Nakahara and K. Kimura, Langmuir 2010 (26) 5444-5450.

- 31. S. J. Clup and F. A. Beland, J. Am. Coll. Toxicol. 1996 (15) 219-238.
- 32. S. Srivastava, R. Sinha and D. Roy, Aquat. Toxicol. 2004 (66) 319-329.
- 33. K. V. K. Rao, Toxicol. Lett. 1995 (81) 107-113.
- 34. B. Bose, L. Motiwale and K. V. K. Rao, Cancer. Lett. 2005 (230) 260-270.
- 35. E. G. Synderwine, R. Sinha, J. S. Felton and L. R. Ferguson, Mutat. Res. Fundam. Mutat. Res. Fundam. Mol. Mech. Mutagen. 2002 (506-507) 1-8.
- 36. N. Daneshvar, A. R. Khataee, M. H. Rasoulifard and M. Pourhassan, J. Hazard. Mater. 2007 (143) 214–219.
- 37. V. Bennett and A. J. Baines, Physiol. Rev. 2001 (81) 1353–1392.
- 38. B. Machnicka, A. Czogalla, A. Hryniewicz-Jankowska, D. M. Boguslawska, R. E. Heger and A. F. Sikorski, Biochim. Biophys. Acta. 2014 (1838) 620-634.
- 39. M. Patra, C. Mukhopadhyay and A. Chakrabarti, PLoS One 2015 (10) e0116991.
- 40. G. E. Begg, M. B. Morris and G. B. Ralston, Biochemistry 1997, (36) 6977–6985.
- 41. J. R. Glenney, J. P. Glenney and K. Weber, J. Biol. Chem. 1982 (257) 9781–9787.
- 42. Q. Li and L. W. Fung, Biochemistry 2009 (48) 206–215.
- S. Mehaboob, Y. Song, M. Weitek, F. Long, B. P. Santarsieo, M. E. Jhonson and L. W. M. Fung, J. Biol Chem. 2010 (285) 14572–14584.
- 44. X. An, X. Zhang, M. Salomao, X. Guo, Y. Yang, Y. Wu and N. Mohandas, Biochemistry 2006 (45) 13670–13676.
- 45. W. Diakowski and A. F. Sikorski, Biochim. Biophys. Acta. 2002 (1564) 403–411.
- D. Ziemnicka-Kotula, J. Xu, H. Gu, A. Potempska, K. S. Kim and E. C. Jenkins et al. J. Biol. Chem. 1998 (273) 13681–92.
- 47. J. Hu, D. Ziemnicka, J. Scalia and L. Kotula, Brain Res. 2001 (898) 171–177.

- 48. J. Xu, D. Ziemnicka, G. S. Merz and L. Kotula, J. Cell. Sci. 2000 (21) 3805–3814.
- 49. T. Pawson and J. D. Scott, Science 1997 (278) 2075–2080.
- 50. B. J. Mayer, R. Ren, K. L. Clark and D. Baltimore Cell 1993 (73) 629–630.
- 51. R. J. Haslam, H. B. Koide and B. A. Hemmings Nature 1993 (363) 309–310.
- 52. J. L. Pauly, R. B. Bankert and E. A. Repasky, J. Immunol. 1986 (136) 246–53.
- 53. T. L. Brown, S. Patil, C. D. Cianci, J. S. Morrow and P. H. Howe, J. Biol. Chem. 1999 (274) 23256–23262.
- K. K. Wang, R. Posmantur, R. Nath, K. McGinnis, M. Whitton and R.V. Talanian, et al.
 J. Biol. Chem. 1998 (273) 22490–22497.
- 55. S. J. Martin, G. A. O'Brien, W. K. Nishioka, A. J. McGahon, A. Mahboubi and T. C. Saido, et al. J. Biol. Chem.1995 (270) 6425–6428.
- 56. A. Lee, J. S. Morrow and V. M. Fowler, J. Biol. Chem. 2001 (276) 20735–20742.
- 57. E. A. Slee, C. Adrain and S. J. Martin J. Biol. Chem. 2001 (27) 7320-7326.
- 58. M. O. Li, M. R. Sarkisian, W. Z. Mehal, P. Rakic and R. A. Flavell, Science **2003**, *302*, 1560–1563.
- 59. R. M. Friedlander, N. Engl. J. Med. 2003 (348) 1365–1375.
- 60. A. Czogalla and A. F. Sikorski, Cell. Mol. Life. Sci. 2005 (62) 1913–1924.
- 61. C. W. Gourlay and K. R. Ayscough, Nat. Rev. Mol. Cell. Biol. 2005, 6, 583–589.
- 62. P. M. Dubielecka, B. Jazwiec, S. Potoczek, T. Wro'bel, J. Miloszewska, O. Haus, K. Kuliczkowski and A. F. Sikorski, Biochem. Pharmacol. 2005 (69) 73–85.
- 63. S. Majee, D. Dasgupta and A. Chakrabarti, Eur. J. Biochem. 1999 (260) 619–626.
- 64. P. M. Dubielecka, A. Trusz, W. Diakowski, M. Grzybek, A. Chorzalska, B. Jazwiec, M. Lisowski, A. Jezierski and A. F. Sikorski, Mol. Membr. Biol. 2006 (23) 235–243.

- 65. A Chakrabarti, S Bhattacharya, S Ray and M Bhattacharyya. Biochem. Biophys. Res. Commun. 2001 (282) 1189-1193.
- 66. M. Bhattacharyya, S. Roy, S. Bhattacharyya, and A. Chakrabarti, J. Biol. Chem. 2004 (279) 5580–5588.
- 67. A. Chakrabarti and M. Patra, Biochim. Biophys. Acta. 2015 (1848) 821–832.
- 68. J. R. Lakowicz, Principle of fluorescence Spectroscopy; 3rd ed. New York: Springer Science + Business Media: 2006, pp 63-606.
- 69. M. R. Eftink and C. A. Ghiron, Anal. Biochem. 1981 (114) 199-227.
- 70. W. Parker and P. S. Song, Biophys. J. 1992 (61) 1435-1439.
- 71. W. C. Jr. Johnsonm, Annu. Rev. Biophys. Biophys. Chem. 1988 (17)145-166.
- 72. E. Lissi and E. Abuin, J. Fluorescence 2011 (21) 1831-1833.
- 73. W. L. Jorgensen and J. T. Rives, J. Am. Chem. Soc. 1988 (110) 1657–1666.
- 74. M. Patra, M. Mitra, A. Chakrabarti and C. Mukhopadhyay, J. Biol. Mol. Struct. Dyna. 2013 (32) 852-865.
- G. M. Morris, R. Huey, W. Lndstrom, M. F. Sanner, R. K. Belew, D. S. Goodsell and A. J. Olson, J. Comput. Chem. 2009 (30) 2785–2791.
- 76. W. L. Delano, Pymol: An open source for molecular graphics tool. San Carlos; CA: De Lano Scientific; 2002.
- 77. S. Tabassum, W. M. Al-Asbahy, M. Afzal, F. Arjmand and R. H. Khan, Mol. Biosyst. 2012 (8) 2424-2433.
- 78. U. Anand, C. Jash, R. K. Boddepalli, A. Shrivastava and S. Mukharjee, J. Phys. Chem. B 2011 (115) 6312-6320.
- 79. P. D. Ross and S. Subramanian, Biochemistry 1981 (20) 3096-3102.

- 80. J. B. F. Lloyd, Natl. Phy. Sci. 1971 (231) 64-65.
- 81. A. Chakrabarti, D. Bhattacharya, S. Deb and M. Chakraborty, PloS One 2013 (8) e81820.
- 82. J. Zhang, S. Zhuang, C. Tong and W. Liu, J. Agric. Food Chem. 2013 (61) 7203-7211.
- 83. K. Saksela, P. Permi, K. Saksela and P. Permi, FEBS. Lett. 2012 (586) 2906–2614.
- 84. E. Kellenberger, J. Rodrigo, P. Muller and D. Rognan, Proteins. 2004 (57) 225-242.

Figure Captions:

- **Fig 1:** Fluorescence emission spectra of erythroid (a) and non-erythroid spectrin (b) upon excitation at 295 nm, pH 8.0 and Temp 298°K in the presence of different concentration malachite green (MG). Down arrow indicates the quenching of tryptophan fluorescence of both proteins with increasing concentration of MG; (c) and (d) indicate the shift in λ_{em} with increasing concentrations of MG for erythroid and non-erythroid spectrin respectively.
- **Fig 2:** The Stern-Volmer plot describing (a) erythroid (b) non-erythroid spectrin Trp residue quenching at pH=7.8 caused by the association of MG. Fluorescence emission intensity was recorded at 338 nm.
- **Fig 3:** Malachite green binding isotherm in 10 mM Tris 20 mM KCl pH=7.8. Plot shows normalized increase in fluorescence against the concentration of (a) erythroid (b) non-erythroid spectrin. Below figure indicates the association constant plot describing Trp residue quenching of (c) erythroid (d) non-erythroid spectrin at pH=7.8 caused by MG conjugation
- **Fig 4:** van't Hoff plot for the molecular recognition of MG by erythroid and non-erythroid spectrin in Tris-HCl buffer, pH=7.8.
- **Fig 5:** Effect of malachite green on the synchronous spectra ($\Delta\lambda$ =60 nm) for Trp residues of (a) erythroid (b) non-erythroid spectrin. Down arrow indicates the quenching of tryptophan fluorescence of both proteins with increasing concentration of MG.

- **Fig 6:** Far UV CD spectra of(a) erythroid (b) non-erythroid spectrin complex with MG (15 μM).
- **Fig 7:** Stren volmer acrylamide quenching plot of (a) erythroid spectrin (b) non-erythroid spectrin in the presence and absence MG.
- **Fig 8:** Energy minimized complex of MG with the self association (a) and SH3 domains (b) of (left panel) erythroid (right panel) non-erythroid spectrin.

Supporting information

- **Fig S1:** SDS-Polyacrylamide Gel Electrophoresis of erythroid spectrin on 7.5% and non-erythroid spectrin on 8% gel.
- **Fig S2:** Energy minimized complexes of the MG with the N terminal domain and ankyrin binding of erythroid spectrin (upper panel) and non-erythroid spectrin (lower panel).
- **Table S1:** Stern–Volmer (K_{SV}) and bimolecular quenching constants (k_q) for the molecular recognition of spectrin with MG.
- Table S2: Effect of ionic strength on the binding of erythroid and non-erythroid spectrin.
- **Table S3:** Fluorescence lifetime components of erythroid and non-erythroid spectrin in the presence and absence MG.
- **Table-S4:** Residues of spectrin involved in the binding of malachite green.

Table 1: Apparent dissociation constants (K_d in μM) of MG to erythroid and non-erythroid spectrin at 25°C, estimated by three different methods. The values of stoichiometry are given in parantheses.

Protein	Double-reciprocal	Non-linear curve	Lissi and Abuin
	Plot	Fitting	Plot
Erythroid Spectrin	24.88±5	9±2	15.37±4
	(0.88)	(0.88)	(0.88)
Non-erythroid	34.01±4	10±3	17.49±3
spectrin	(0.88)	(0.88)	(0.88)

Table-2: Thermodynamic parameters associated with binding of MG with erythroid and non-erythroid spectrin in buffer 10 mM Tris and 20 mM KCl at pH=7.8.

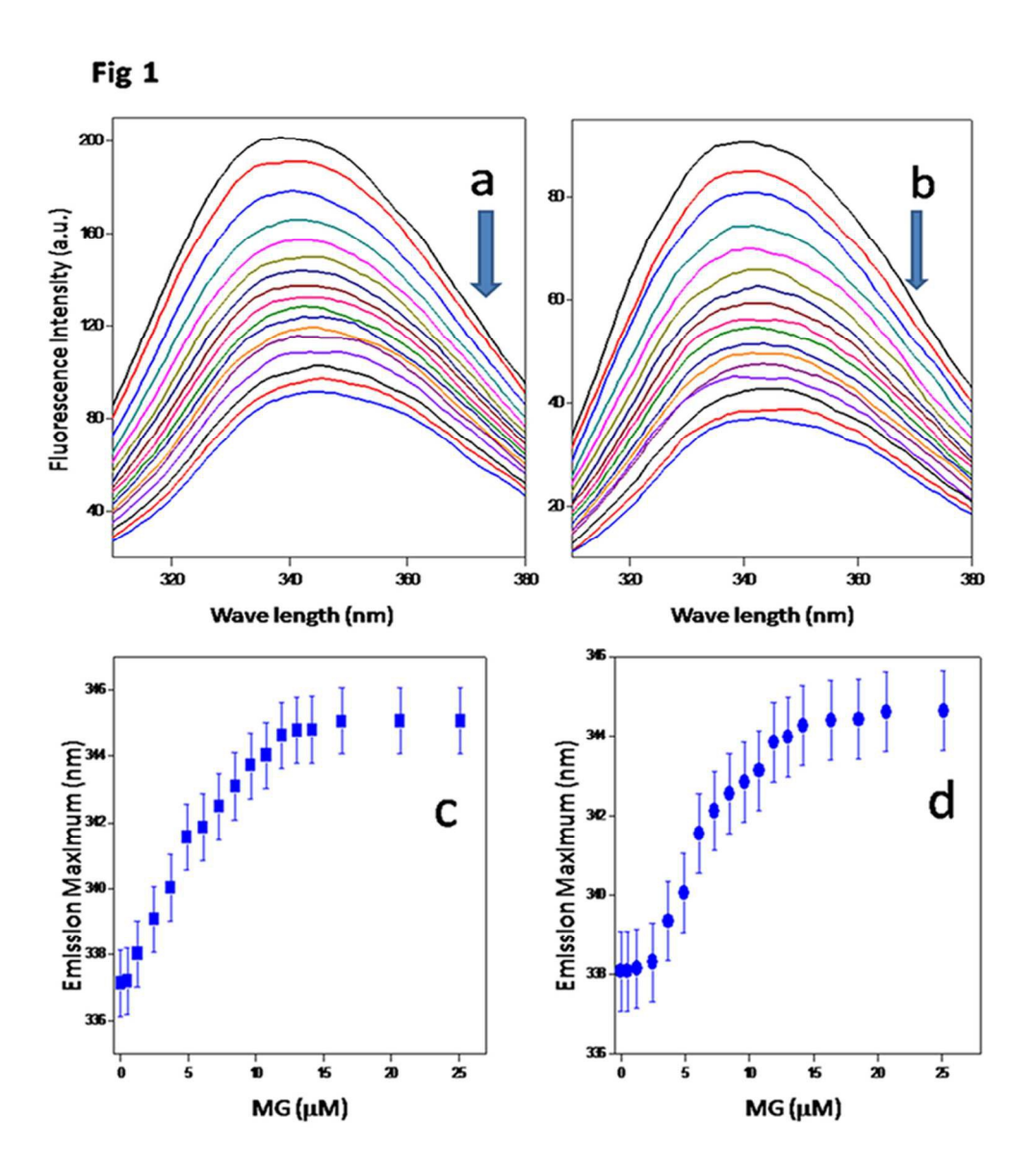
Protein	ΔH (J mol ⁻¹ K ⁻¹)	ΔS (J mol ⁻¹ K ⁻¹)	ΔG (J mol ⁻¹ K ⁻¹)
Erythroid Spectrin	-15.337	39.646	-118.29
Non-erythroid spectrin	-8.156	65.4102	-19.500

Table-3: Stern Volmer quenching constants of erythroid and non-erythroid spectrin in presence and absence of MG.

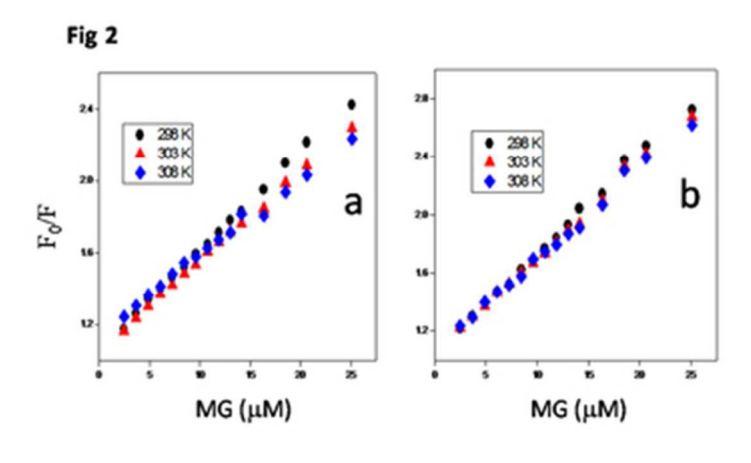
Protein	K _{SV} M ⁻¹ Protein	K _{SV} M ⁻¹ Protein+MG
Erythroid Spectrin	4.6±0.2	3.0±0.3
Non-erythroid Spectrin	4.2±0.2	3.3±0.2

Table-4: Computed binding energies of binding of four different domains of erythroid and non-erythroid spectrin.

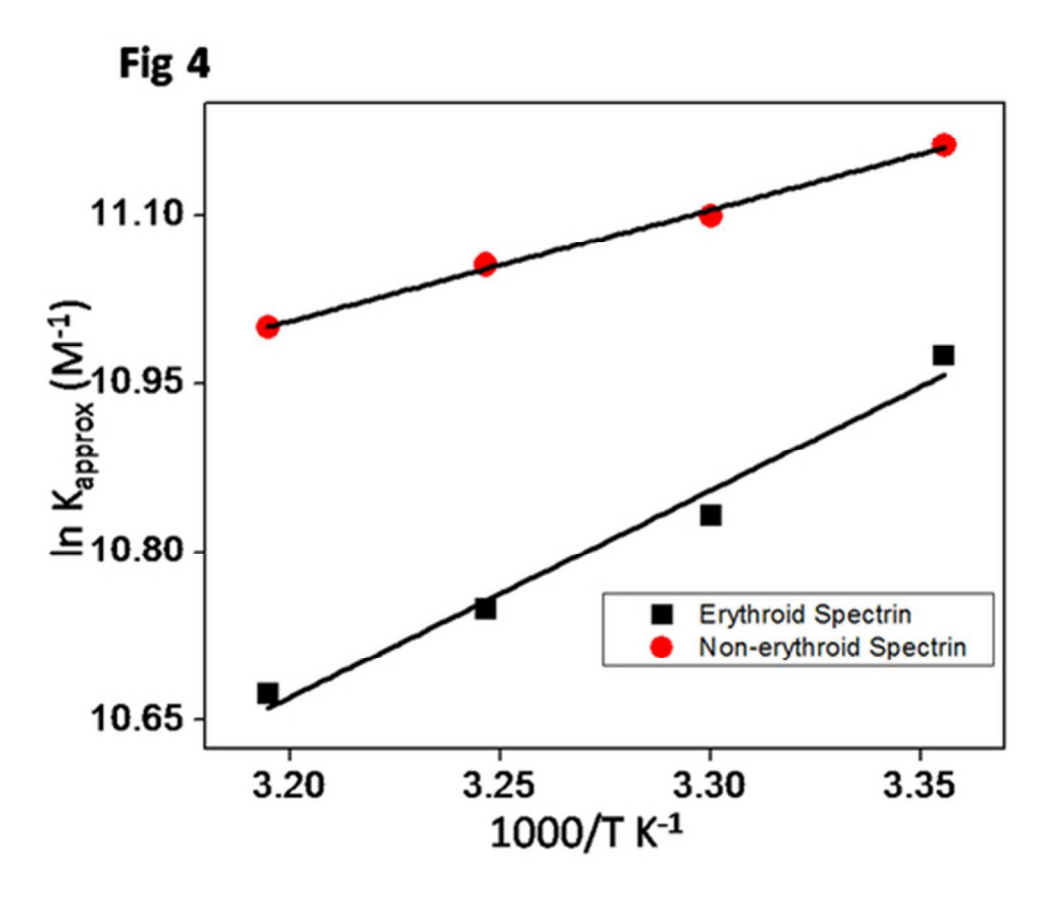
Protein	Domain/Model	MG (interaction energy k- cal/mol)
Erythroid Spectrin	SH3 domain Self association N-terminal of α-spectrin Ankyrin binding domain	-3.94 -0.69 -0.46 0.26
Non-erythroid Spectrin	SH3 domain Self association N-terminal of α-spectrin Ankyrin binding domain	-4.51 -0.27 -0.19 -0.02



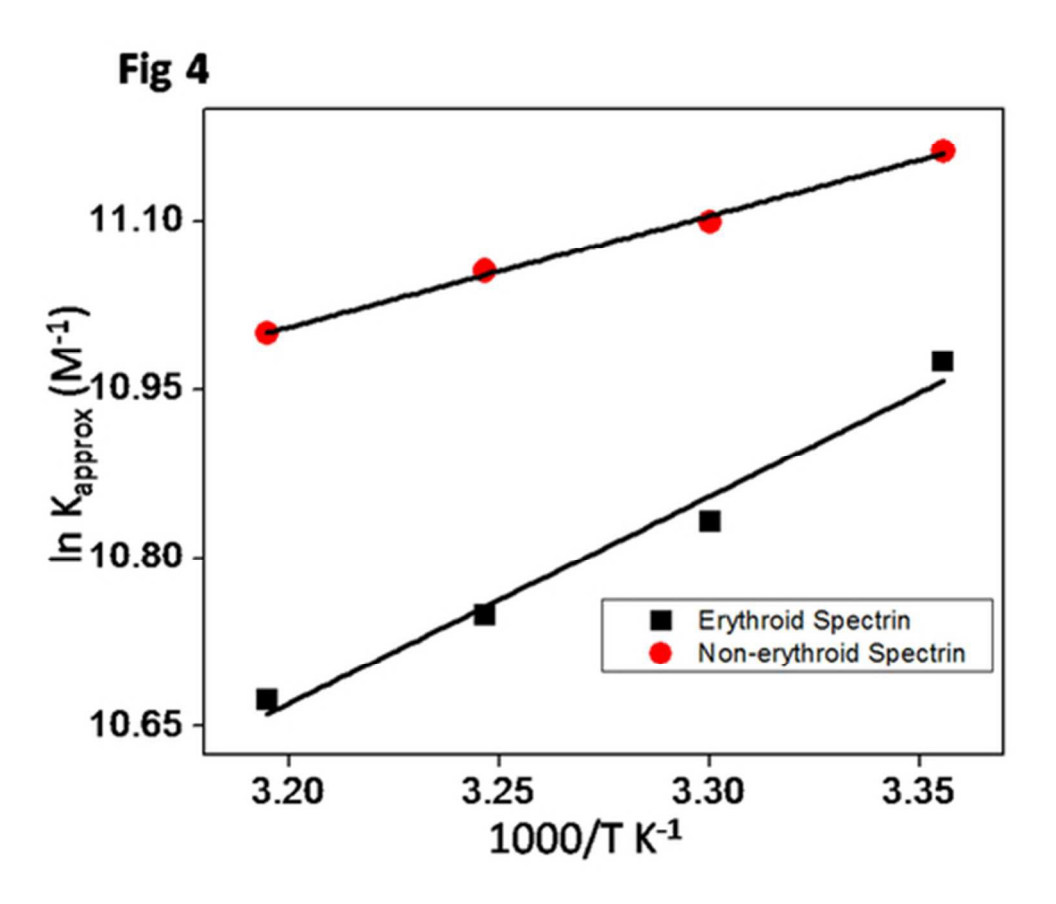
Fluorescence emission spectra 86x99mm (300 x 300 DPI)



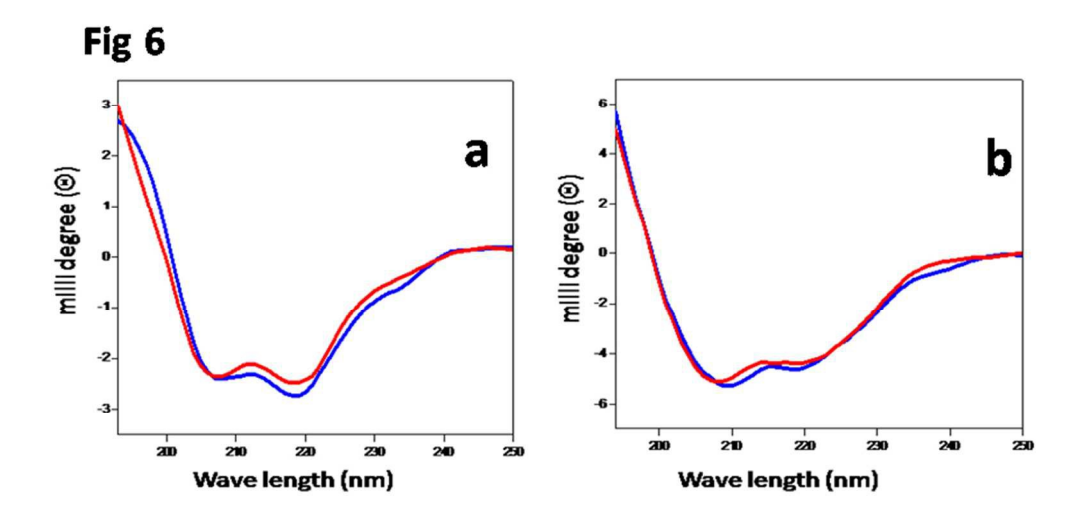
Stern-Volmer plot 29x17mm (300 x 300 DPI)



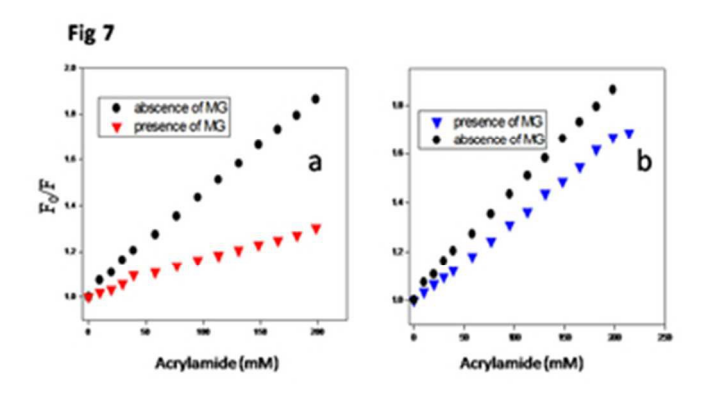
Malachite green binding isotherm 42x35mm (300 x 300 DPI)



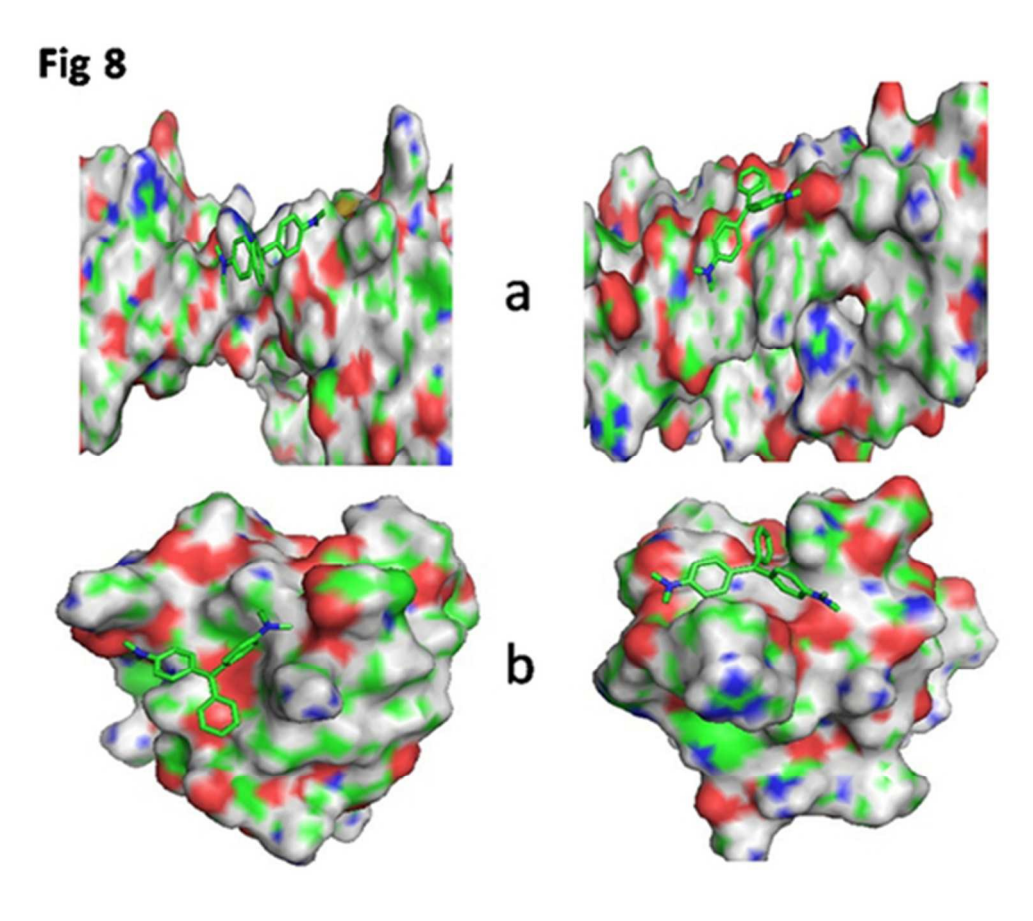
Malachite green binding isotherm 42x35mm (300 x 300 DPI)



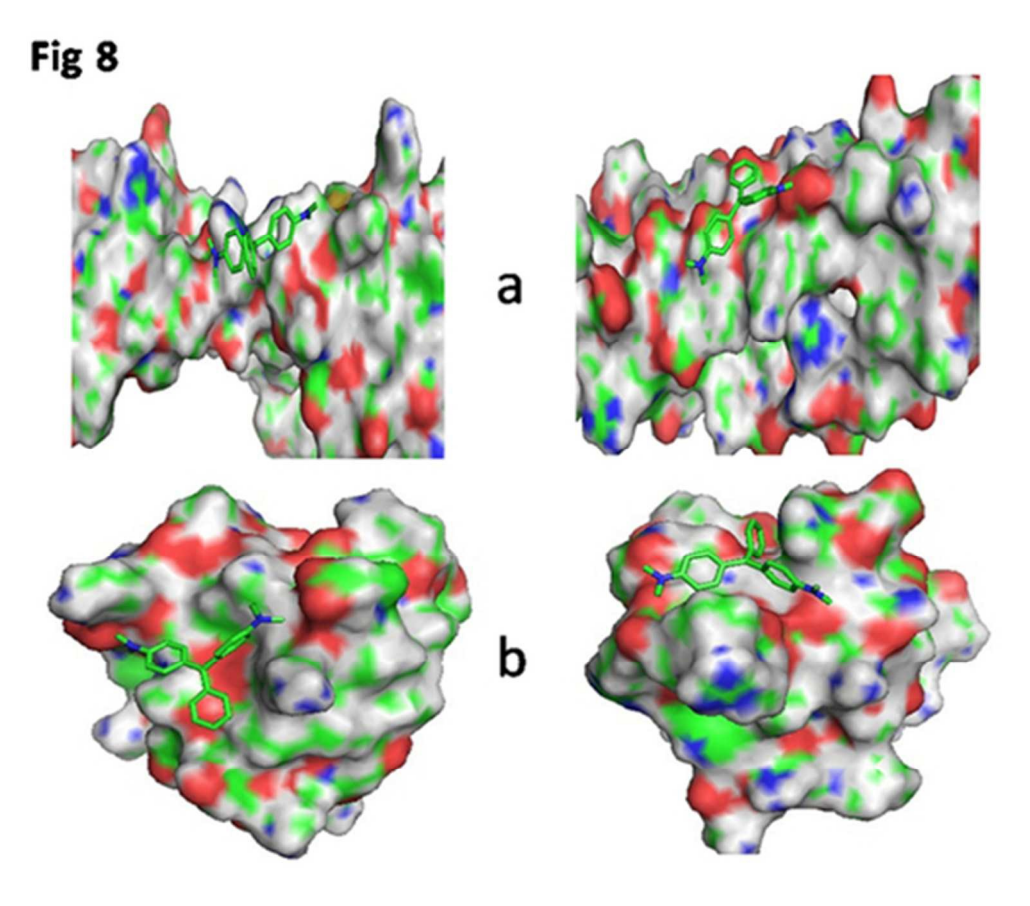
Far UV CD spectra of proteins 236x120mm (96 x 96 DPI)



Stren volmer acrylamide quenching plot of proteins $28x15mm (300 \times 300 DPI)$



Energy minimized complex of MG with proteins 43x37mm (300 x 300 DPI)



Energy minimized complex of MG with proteins 43x37mm (300 x 300 DPI)